Geomechanics and Engineering, *Vol. 22, No. 1 (2020) 11-23*
DOI: https://doi.org/10.12989/gae.2020.22.1.011

A new analytical-numerical solution to analyze a circular tunnel using 3D Hoek-Brown failure criterion

Masoud Ranjbarnia[*1], Nima Rahimpour[1a] and Pierpaolo Oreste[2b]

[1]*Department of Geotechnical Engineering, Faculty of Civil Engineering, University of Tabriz, 29 Bahman Blvd, Tabriz, Iran*
[2]*Department of Environmental, land and infrastructure Engineering, Politecnico di Torino, Corso Duca degli Abruzzi, Torino 24-10129, Italy*

(Received June 8, 2019, Revised April 28, 2020, Accepted May 19, 2020)

Abstract. In this study, a new analytical-numerical procedure is developed to give the stresses and strains around a circular tunnel in rock masses exhibiting different stress-strain behavior. The calculation starts from the tunnel wall and continues toward the unknown elastic-plastic boundary by a finite difference method in the annular discretized plastic zone. From the known stresses in the tunnel boundary, the strains are calculated using the elastic-plastic stiffness matrix in which three dimensional Hoek-Brown failure criterion (Jiang and Zhao 2015) and Mohr-Coulomb potential function with proper dilation angle (i.e., non-associated flow rule) are employed in terms of stress invariants. The illustrative examples give ground response curve and show correctness of the proposed approach.
Finally, from the results of a great number of analyses, a simple relationship is presented to find out the closure of circular tunnel in terms of rock mass strength and tunnel depth. It can be valuable for the preliminary decision of tunnel support and for prediction of tunnel problems.

Keywords: circular tunnel; stress and strain; stiffness matrix; analytical solution; three dimensional Hoek-Brown criterion; stress invariants

1. Introduction

Analytical solutions to obtain stresses and displacements around a tunnel give a good first estimation of tunneling problem potential and so forth make its preliminary design possible in a wide variety of geotechnical engineering conditions. These solutions for the elastic-plastic behavior of rock mass are normally feasible for a circular opening subjected to a hydrostatic in situ stresses. Accordingly, numerous studies have been conducted on this axisymmetric problem. The differences among these works may refer to either (both) considering different rock mass behaviors and failure criterions or (and) employing various solution methods and algorithms.

Regarding the strain softening behavior, Brown *et al.* (1983) were among the first authors who presented an analytical-numerical stepwise procedure for the stresses and displacements around a circular tunnel in the Hoek-Brown media (Fig. 1, where r_i is tunnel radius, r_e is elastic-plastic boundary radius, p_0 is in-situ stress, and σ_r and σ_θ are respectively radial and tangential stresses). This solution involves the discretization of the plastic zone in unknown number of annular rings so that the calculation starts from the unknown elastic-plastic interface towards the tunnel wall by incrementing the tangential strain value for each calculation step, and then computing the corresponding radial strain and the stresses. This solution procedure was modified by Park *et al.* (2008) through considering the effects of elastic strain increments within the plastic region. Lee and Pietruszczak (2008) proposed a finite difference approximate scheme which looks similar to that of Brown *et al.* procedure (1983), but the calculation in each step proceeds in a reverse order. That is, unlike the Brown *et al.* method (1983), the radial stress is firstly calculated in each

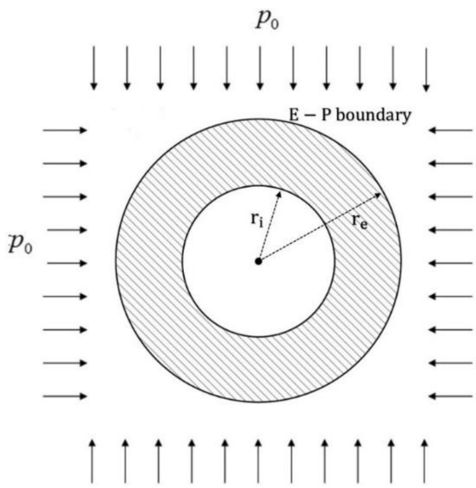

Fig. 1 Schematic Elastic-Plastic radius around the tunnel cavity (Brown *et al.* 1983)

*Corresponding author, Assistant Professor
E-mail: m.ranjbarnia@tabrizu.ac.ir
[a]Master
E-mail: nimarahimpour@yahoo.com
[b]Professor
E-mail: pierpaolo.oreste@polito.it

ISSN: 2005-307X (Print), 2092-6219 (Online)

ring through the stress equilibrium equation (starting from unknown location of elastic-plastic interface to tunnel wall), and the corresponding strains are then found. Wang and Zou (2018) presented a similar finite difference method, but each step of calculation starts with a radius increment. The stress for each annulus is obtained analytically, while the corresponding strain increments is calculated numerically from the compatibility equation by finite difference approximation. Zou *et al.* (2019), like the above-mentioned methods, divided the plastic radius into finite number of annular rings whose thickness were determined internally to satisfy the equilibrium and compatibility equations.

Regarding the other methods of solution for the strain-softening behavior, Alonso *et al.* (2003) formulated the problem to a system of ordinary differential equations which are derived from the usual partial differential equations system. They can be simply numerically solved by a Runge- Kutta- Fehlberg method for generic materials considering failure criterion and the plastic potential or flow rule. Wang *et al.* (2010) proposed a new approach to simulate the strain softening process of stress-strain relationship into a series of brittle and perfectly plastic models. The stresses and strains can be calculated by the available closed form solutions.

However, other efforts have been conducted to study effects of some other aspects on the developed stress and strain around tunnel. These studies might be categorized as

- those focused on rock mass properties e.g. rock mass dilatancy (Alejano and Alonso 2005, Zou *et al.* 2017), non-homogeneity (González *et al.* 2013), full saturation i.e., underwater tunnel (Fahimifar *et al.* 2015, Zou and Wei 2018), spatial characteristics such as the strike and dip angle (Yoo, 2016), both of dip angle and joint spacing of systematic discontinuities (Nikadat and Fatehi Marj 2016), time dependency (creep) Paraskevopoulou and Diederichs 2018, Quevedo and Bernaud 2018)
- those concentrated on rock mass stress- strain behavior e.g., non-linearity of stress- strain relation of softening stage (Ranjbarnia *et al.* 2015), the extension of softening stage in stress- strain relation curve (Alonso *et al.* 2003, Alejano *et al.* 2009, 2010),
- those related to in-situ stress e.g. biaxial in-situ stresses (Zhuang *et al.* 2018), the stress along tunnel axis (Zou and Zheng 2016),
- those considered other issues e.g. inclusion of dead weigtht loading of broken rock on GRC (Zareifard 2019).

Regarding the other stress-strain behavior, some other exact closed form solutions have been presented for the perfectly plastic (FAMA 1993, Panet 1993, Carranza-Torres and Fairhurst 1999) and brittle plastic, stress- strain relation behavior of the rock mass (Carranza-Torres 1998, Carranza-Torres and Fairhurst 1999, Sharan 2003, CarranzaTorres 2004, Park and Kim 2006, Osguii and Oreste 2007, Tu *et al.* 2018, Park 2017).

A literature review shows that there exist adequate techniques to obtain the stresses and strains for tunnels excavated in elasto-plastic materials. However, for the strain softening behavior, it seems that it is worth developing a new approach to give the strains with less calculations in the tunnel wall. Particularly, if this new solution has a readiness to be extended to the case of non-hydrostatic in-situ stress condition, it will be more addressed.

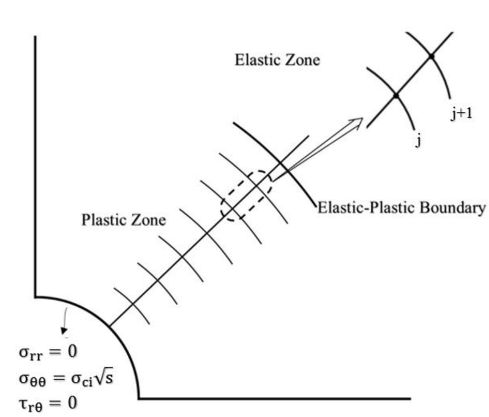

Fig. 2 Mesh generation around the excavated tunnel in hydrostatic stress field condition

This study presents a new analytical solution in which the zone around tunnel is meshed into given number of annular rings. The calculations start from the tunnel wall toward the unknown elastic-plastic boundary (Fig. 2). From the known stresses in tunnel boundary (the shear and radial stresses are null where tangential stress can be found by failure criterion), the strains are calculated using the elastic-plastic stiffness matrix in which an appropriate failure criterion (i.e., 3D Hoek-Brown failure function proposed by Ziang and Zhao 2015) and non-associated flow rule (by using 3D Mohr-Coulomb as potential function) are employed. The calculations are continued to the next known local ring by obtaining its stresses from equilibrium differential equation through using the failure criterion and finite difference method. It continues till to a ring where the stresses of elastic-plastic boundary are obtained. Some illustrative examples are solved to show the correctness of the proposed approach. The distinguished features of presented approach are

- the method is originally three-dimensional; hence for calculation of stiffness matrix, three-dimensional failure criterion and potential function are used. The method of using 3D functions can be treated as the basis for solution of 3D tunnel problems; and
- it is possible to obtain the tunnel convergence at the first step of calculations. In fact, for the calculation of tunnel convergence, it is not required to find the stress and strains around tunnel.

Unlike the other proposed approaches, this one presents a solution method that can be extended to the case of non-hydrostatic in-situ stress condition, since the required calculations start from tunnel boundary toward elastic-plastic boundary. Furthermore, in non-hydrostatic in-situ stress condition, the elastic-plastic interface is not circular anymore, and associated calculations of the other proposed methods (which are performed by using simple circular meshes) cannot be started from that boundary.

Finally, based on a great number of analyses by the presented approach, a simple relationship for calculation of a circular tunnel closure on the basis of the rock mass strength and tunnel depth is given. It can be valuable for the preliminary decision of using a tunnel support and for the prediction of the presence of tunnel squeezing problems (Hoek and Marinos 2000).

2. Problem definitions and General assumptions

Assuming that a circular tunnel is excavated in a continuous, homogeneous, isotropic, initially elastic rock mass subjected to a hydrostatic stress p_0 (i.e., the plane strain condition), a circular plastic zone is generally developed around a tunnel, and in-situ stresses are redistributed in terms of the radial and tangential stresses as the minor and the major principal stresses (Fig. 1).

In the plastic zone, the stresses are limited by Hoek-Brown failure criterion (Fig. 3) which can be expressed in term of the stress invariants. For the modified Hoek-Brown failure criterion (Fig. 4), the stress invariants in three-dimensional space are (Jiang and Zhao 2015)

$$f(\{\sigma'\},\{m\}) = \frac{1}{m\sigma_{ci}^{1/a-1}}\left(\sqrt{3J_2'}\right)^{1/a} + \frac{A(\theta)}{\sqrt{3}}\sqrt{J_2'} - \frac{s\sigma_{ci}}{m} - \sigma_m' = 0 \tag{1}$$

where the parameters J_2', θ and σ_m' are the stress invariants defined as (Jiang and Zhao 2015, Jiang and Xie 2012)

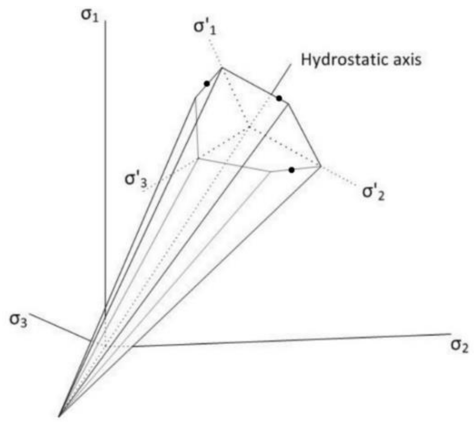

Fig. 3 The original Hoek- Brown failure criterion in principal stresses spaces

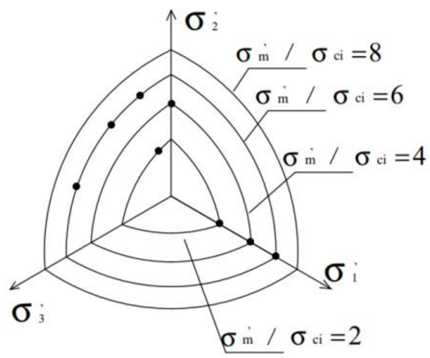

Fig. 4 Stress position in the modified three-dimensional Hoek-Brown criterion (Jiang and Zhao 2015)

$$\sigma_m' = \frac{1}{3}(\sigma_{11} + \sigma_{22} + \sigma_{33}) \tag{2}$$

$$J_2' = \frac{1}{6}[(\sigma_{11} - \sigma_{22})^2 + (\sigma_{11} - \sigma_{33})^2 + (\sigma_{22} - \sigma_{33})^2] \tag{3}$$

$$\theta = \mathrm{Arccos}\left(\frac{2\sigma_{11} - \sigma_{22} - \sigma_{33}}{2\sqrt{3}\sqrt{J_2'}}\right) \quad 0 \le \theta \le \frac{\pi}{3} \tag{4}$$

The parameter θ is the Lode angle depending on the stresses values at each loading step. σ_{11}, σ_{22} and σ_{33} are the principal stresses, and $A(\theta)$ is (Jiang and Zhao 2015) (Fig. 4).

$$A(\theta) = 2\cos\left(\frac{\pi}{3} - \theta\right) \tag{5}$$

In above equations, σ_{ci} is the uniaxial compressive strength of intact rock material, and parameters, s and a are the Hoek-Brown rock mass constants depending on rock mass nature and its geotechnical conditions, and can be calculated by Geological Strength Index (GSI) of rock mass. It is a characterization tool for assessing engineering properties of rock mass. For poor rock mass, moderate, and good rock mass, it is respectively: $GSI < 25$, $25 < GSI < 75$, and $GSI > 75$ (Hoek and Brown 1997).

For the elastic-perfectly plastic and elastic-brittle plastic stress-strain relationship, the rock mass constants are values corresponding to before failure (i.e., m_p and s_p) and to residual conditions (i.e., m_r and s_r), respectively; but for the strain softening behavior, they depend upon the value of principal plastic strains (Brown *et al.* 1983) i.e.,

$$m_{sof} = m_p - (m_p - m_r)\frac{\eta}{\eta^*} \tag{6a}$$

$$s_{sof} = s_p - (s_p - s_r)\frac{\eta}{\eta^*} \tag{6b}$$

where η is the softening parameter as (Alonso *et al.* 2003)

$$\eta = \varepsilon_{11}^p - \varepsilon_{33}^p \tag{7}$$

and η^* is the critical softening parameter that can be obtained from triaxial compression tests or from the analytical method by Alejano *et al.* (2009). The strains ε_{11}^p and ε_{33}^p are the plastic principal strains which will be calculated by the approach presented in the next sections.

For intact rock, as the special case, the parameter $a = 0.5$; then Eq. (1) is simplified, and the parameter $\frac{\sqrt{J_2'}}{\sigma_{ci}}$ is introduced which can be explicitly derived by Eq. (8)

$$\frac{\sqrt{J_2'}}{\sigma_{ci}} = \frac{1}{6}\left[-\frac{m_i}{\sqrt{3}}A(\theta) + \sqrt{\frac{{m_i}^2}{3}A^2(\theta) + 12\left(m_i\frac{\sigma_m'}{\sigma_{ci}} + s_i\right)}\right] \tag{8}$$

where m_i and s_i are the constants for intact rock.

To calculate the strains in the plastic zone, an appropriate potential function is needed. The previous studies proved that directions of plastic strains rate do not coincide to those of stresses. That is, the non-associated flow rule must be used, and a proper stress potential function which involves material properties and reflects volumetric plastic strain should be employed.

If the Hoek-Brown function is selected as the potential function, calibration of the material properties associated to plastic volumetric strains parameters (i.e., dilation angle) is too difficult. Therefore, the Mohr-Coulomb function was chosen, which is more similar to the Hoek- Brown function in the three-dimensional spaces of principal stresses (the irregular hexagon surface of both functions, see Fig. 4). The three-dimensional Mohr-Coulomb stress function is (Griffiths and Willson 1986),

$$p(\{\sigma'\},\{k\}) = J_2' - (a_{pp} + \sigma_m')g_{pp}(\theta) = 0 \tag{9}$$

where

$$g_{pp}(\theta) = \frac{\sin\psi}{\cos\theta + \frac{\sin\theta\sin\psi}{\sqrt{3}}} \tag{10}$$

and

$$a_{pp} = \left(\frac{c'}{\tan\varphi'} + {\sigma_m'}^*\right)\frac{g(\theta^*)}{g_{pp}(\theta^*)} - {\sigma_m'}^* \tag{11}$$

where

$$g(\theta) = \frac{\sin\varphi'}{\cos\theta + \frac{\sin\theta\sin\varphi'}{\sqrt{3}}} \tag{12}$$

where the parameters c' and φ' are equivalent cohesion and friction angle of the rock mass calculated by (Hoek *et al.* 2002), ψ is the dilation angle which is $\frac{\varphi'}{8}$, and $\frac{\varphi'}{4}$ for the weak and normal rock mass, respectively (Hoek and Brown 1997). Superscript * indicates the current stress state.

The relation between the strains and stresses is expressed as

$$\sigma_{ij} = D_{ijkl}^{ep}\varepsilon_{kl} \tag{13}$$

where parameter D^{ep} is the stiffness matrix introduced by

$$[D^{ep}] = [D^e] - \frac{[D^e]\left[\frac{\partial p}{\partial\sigma}\right]\left[\frac{\partial f}{\partial\sigma}\right]^T[D^e]}{\left[\frac{\partial f}{\partial\sigma}\right]^T[D^e]\left[\frac{\partial p}{\partial\sigma}\right] + H} \tag{14}$$

where D^e is the elastic stiffness matrix which its components are dependent upon Elasticity Modulus and Poisson's ratio. It can be calculated by Theory of Elasticity references. H is the strain softening parameter and can be found via the following equation (Potts *et al.* 2001), and f and p indicate the failure and potential functions, respectively.

$$H = -\left[\frac{\partial f}{\partial\varepsilon^p}\right]\left[\frac{\partial p}{\partial\sigma}\right] \tag{15}$$

The details of obtaining of Eq. (15) for this problem will be given in Section 3.

3. The solution method

3.1 Plastic zone

If it is assumed the plane strain condition exists, the stress tensor components will be (Lai *et al.* 2009)

$$\sigma_{ij} = \begin{bmatrix}\sigma_{11}\\ \sigma_{22}\\ \sigma_{33}\\ \sigma_{13}\end{bmatrix} \tag{16}$$

and in the polar coordinate under hydrostatic stress condition, it is

$$\sigma_{ij} = \begin{bmatrix}\sigma_{\theta\theta}\\ \sigma_{yy}\\ \sigma_{rr}\\ \sigma_{r\theta}\end{bmatrix} \tag{17}$$

where σ_{yy} is the normal component of the stress tensor along tunnel axis and is constant during tunnel advancement in hydrostatic in-situ stress condition (Brown *et al.* 1983). The strain tensor components appear in the same sequence of stress i.e.,

$$\varepsilon_{ij} = \begin{bmatrix}\varepsilon_{\theta\theta}\\ \varepsilon_{yy}\\ \varepsilon_{rr}\\ \varepsilon_{r\theta}\end{bmatrix} \tag{18}$$

The calculation procedures start from the tunnel wall with known stresses as

$$\begin{gathered}\sigma_{rr} = 0\\ \sigma_{r\theta} = 0\\ \sigma_{\theta\theta} = s^a\ \sigma_{ci}\end{gathered} \tag{19}$$

To calculate strains, Eq. (13) should be rewritten in an incremental form as

$$d\sigma_{ij} = D_{ijkl}^{ep}d\varepsilon_{kl} \tag{20}$$

There is a redistribution of the in-situ stresses due to tunnel face excavations. As a result, the magnitudes of radial and tangential stresses gradually vary from their initial value p_0 to final values in Eq. (19). Accordingly, in this solution, the radial stress is reduced in n increments. For the elastic condition when the radial stress varies from p_0 to σ_{re} (value of radial stress when plastic strains start to occur), one increment is only considered while for the plastic condition when it varies from σ_{re} to zero, in which the behavior is non-linear, n-1 increments are employed. Then, the radial stress increment is

$$d\sigma_{rr} = \sigma_{re}/(n-1) \tag{21}$$

while

$$d\sigma_{yy} = 0 \quad , \quad d\sigma_{r\theta} = 0 \tag{22}$$

and the corresponding increment of tangential stress is found by the failure criterion

$$d\sigma_{\theta\theta} = \sigma_{\theta\theta(j+1)} - \sigma_{\theta\theta(j)} \tag{23}$$

To compute each strain increment, the stiffness matrix i.e., D^{ep}must be calculated. For this purpose, parameter H in Eq. (15) is obtained for the plane strain condition by

$$H = -\left[\frac{\partial f}{\partial \varepsilon^p}\right]_{1\times4}\begin{bmatrix}\frac{1}{3}(2\sigma_{11}-\sigma_{22}-\sigma_{33})+\frac{\left(2\sqrt{3}\sin(\psi)\right)}{3(\sin(\psi)-\ 3)}\\ \frac{1}{3}(2\sigma_{22}-\sigma_{11}-\sigma_{33})+\frac{\left(2\sqrt{3}\sin(\psi)\right)}{3(\sin(\psi)-\ 3)}\\ \frac{1}{3}(2\sigma_{33}-\sigma_{22}-\sigma_{11})+\frac{\left(2\sqrt{3}\sin(\psi)\right)}{3(\sin(\psi)-\ 3)}\\ 0\end{bmatrix} \tag{24}$$

where

$$\frac{\partial f}{\partial \varepsilon^p} = \left[\frac{\partial f}{\partial \sigma}\right]^T \times \frac{\partial \sigma}{\partial \varepsilon^p} \tag{25}$$

In fact, D^{ep} is a constant for each step of increment and can be calculated with previous step characteristic. Furthermore, using non-associated flow rule leads the components of the elastic-plastic stiffness matrix not to be symmetric.

For the strain softening behavior (Fig. 5), the stresses and so forth D^{ep} depend upon the strains which are still unknown, and the problem is solved by an implicit way. After calculation of each strain increment, summing of all increments gives the total strains.

For the next ring calculation, the stresses must be satisfied in the equilibrium equations

$$\frac{\partial\sigma_{rr}}{\partial r} + \frac{1}{r}\left(\frac{\partial\sigma_{r\theta}}{\partial\theta}\right) + \frac{1}{r}(\sigma_{rr} - \sigma_{\theta\theta}) = 0 \tag{26a}$$

$$\frac{\partial\sigma_{r\theta}}{\partial r} + \frac{1}{r}\left(\frac{\partial\sigma_{\theta\theta}}{\partial\theta}\right) + \frac{2\sigma_{r\theta}}{r} = 0 \tag{26b}$$

or in a hydrostatic in-situ stress condition

$$\frac{d\sigma_{rr}}{dr} + \frac{1}{r}(\sigma_{rr} - \sigma_{\theta\theta}) = 0 \tag{27}$$

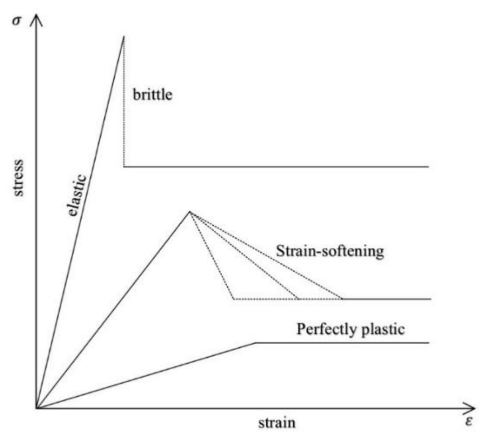

Fig. 5 Different stress- strain behaviors (Hoek and Brown 1997)

Assuming the circular meshes are very small enough, the Eq. (27) might be approximated as

$$\frac{\sigma_{rr(i+1)} - \sigma_{rr(i)}}{r_{(i+1)} - r_{(i)}} + \frac{\bar{\sigma}_{rr} - \bar{\sigma}_{\theta\theta}}{\bar{r}} = 0 \tag{28}$$

in which

$$\bar{\sigma}_{rr} = \frac{1}{2}\left(\sigma_{rr(i+1)} + \sigma_{rr(i)}\right) \tag{29}$$

$$\bar{\sigma}_{\theta\theta} = \frac{1}{2}\left(\sigma_{\theta\theta(i+1)} + \sigma_{\theta\theta(i)}\right) \tag{30}$$

$$\bar{r} = \frac{1}{2}\left(r_{(i+1)} + r_{(i)}\right) \tag{31}$$

where

$$r_{(i+1)} = r_{(i)} + dr \tag{32}$$

(i indicates rings number)

Assuming

$$dr = 0.01r_a \ \ (\ r_a \text{ is the tunnel radius}) \tag{33}$$

and using the equilibrium equation as well as the failure criterion, the value of radial and tangential stresses at the new ring are obtained. Again, the stresses vary from their initial value p_0 to the new values by using failure criterion and (28)-(32) in an incremental way, and the remaining calculation process is carried out as the similar way carried out for tunnel wall.

These calculations are repeated for all rings until the radial stress approximately equals to that of elastic-plastic boundary which is discussed at the next section. The corresponding r is the elastic-plastic radius.

It can be seen that there is no need to calculate the stresses and strains in all rings around tunnel for calculation tunnel convergence in tunnel wall, and hence, less calculations are required in comparison with other approaches.

Note that in non-hydrostatic stress condition, the number of steps (or say rings) to reach elastic-plastic boundary in each point of tunnel boundary is not identical, and hence, the plastic zone is not circular. Furthermore, the medium around tunnel is discretized tangential and radial directions, both equilibrium Eq. (26) are employed, and the radial stress in elastic-plastic boundary is different from that obtained in hydrostatic in-situ stress.

3.2 Elastic zone

To solve the equilibrium equation in the elastic region (shown in Fig. 1), the Airy stress function can be used. For this purpose, the field stress is considered in terms of Spherical stresses with the following Airy stress function (Sadd 2009)

$$\varphi = A_1\ln(r) + B_1 r^2\ln(r) + C_1 r^2 + D_1 \tag{34}$$

where A_1, B_1, C_1, and D_1 are the coefficients that can be calculated with boundary conditions.

This function must satisfy equilibrium equations and strain compatibility in plane strain. The stresses are found

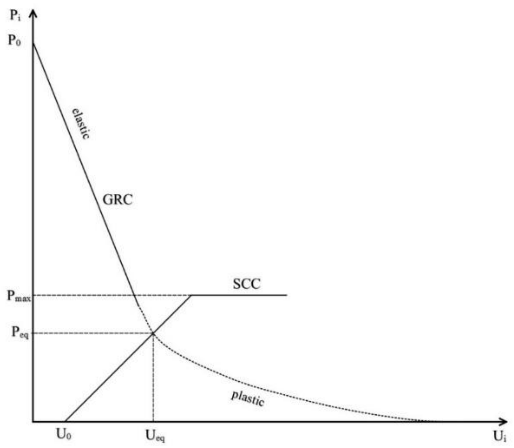

Fig. 6 Schematic of convergence confinement method

Table 1 Characteristic of different rock mass quality (Alejano *et al.* 2010)

	GSI=75	GSI=60	GSI=50	GSI=40	GSI=25
Specific weight (kN/m^3)	25	25	25	25	25
Tunnel depth (m)	600	600	600	600	600
Diameter (m)	6	6	6	6	6
GSI^{peak}	75	60	50	40	25
GSI^{res}	40	35	30	27	25
p_0 (MPa)	15	15	15	15	15
Intact Rock Strength, σ_{ci} (MPa)	75	75	75	75	75
m_p	4.09	2.397	1.677	1.173	0.687
s_p	0.0622	0.0117	0.0039	0.0013	0.0002
m_r	1.173	0.981	0.821	0.737	0.687
s_r	0.0013	0.0007	0.0004	0.0003	0.0002
ψ_p (deg) = ψ_r (deg)	9.42	5.75	3.81	1.72	0
E (GPa)	36.51	15.4	8.66	4.87	2.053
ν	0.25	0.25	0.25	0.25	0.25
η^* ($\times 10^{-3}$)	0.81	1.1	2.6	9.9	Infinity

by (Sadd 2009)

$$\sigma_r = \frac{1}{r}\left(\frac{\partial\varphi}{\partial r}\right) + \frac{1}{r^2}\left(\frac{\partial^2\varphi}{\partial\theta^2}\right) \tag{35}$$

$$\sigma_\theta = \frac{\partial^2\varphi}{\partial\theta^2} \tag{36}$$

$$\tau_{r\theta} = -\frac{\partial}{\partial r}\left(\frac{1}{r}\frac{\partial\varphi}{\partial\theta}\right) \tag{37}$$

Substituting Eq. (34) into Eqs. (35)-(37) with the following boundary conditions

$$\text{At } r = r_e \rightarrow \sigma_r = \sigma_{re} \quad \text{and} \quad \tau_{r\theta} = 0 \ ;$$

$$\text{At } r = \infty \rightarrow \sigma_r = p_0 \quad \text{and} \quad \tau_{r\theta} = 0$$

where σ_{re} is radial stress in the elastic-plastic boundary. Substituting the values of radial and tangential stresses at $r = r_e$ in the two-dimensional Hoek-Brown failure equation at moment of failure gives

$$2(p_0 - \sigma_{re}) = \sigma_{ci}\left(m_p\frac{\sigma_{re}}{\sigma_{ci}} + s_p\right)^a \tag{38}$$

A numerical technique e.g., the Newton-Raphson method can be applied to Eq. (38) to obtain σ_{re} . However, an exact solution is possible when $a = 0.5$ (which is appropriate for good to moderate rock mass) i.e.,

$$\sigma_{re} = p_0 - M\sigma_{ci} \tag{39}$$

in which

$$M = \frac{1}{2}\left[\left(\frac{m_p}{4}\right)^2 + m_p\frac{p_0}{\sigma_{ci}} + s_p\right]^{\frac{1}{2}} - \frac{m_p}{8} \tag{40}$$

These equations were previously presented by Brown *et al.* (1983).

3.3 The convergence confinement method (CCM) and ground reaction curve (GRC)

The convergence-confinement method is part of the

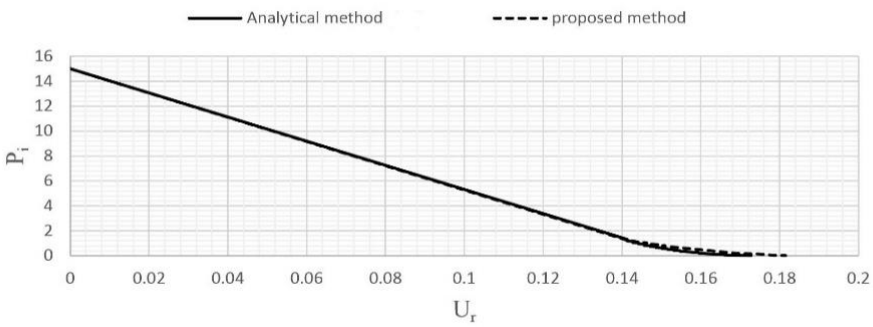

(a) GSI = 75

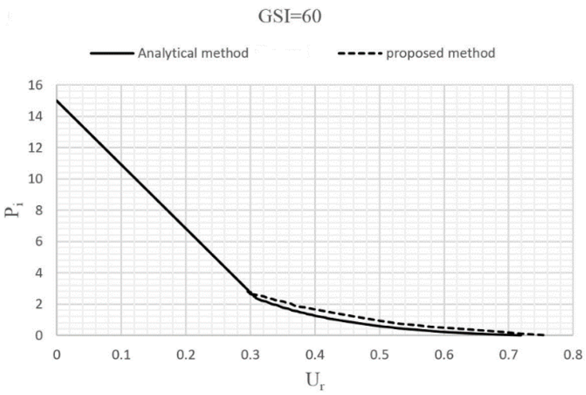

(b) GSI = 60

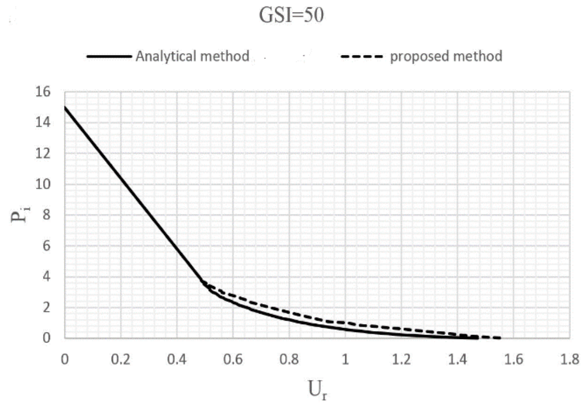

(c) GSI = 50

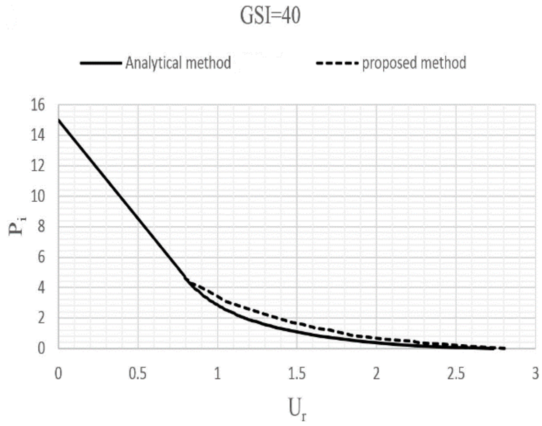

(d) GSI = 40

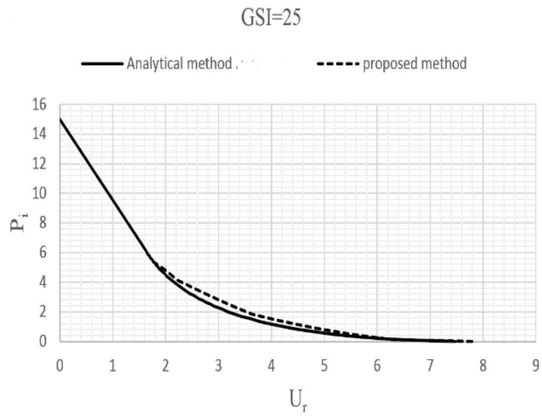

(e) GSI = 25

Fig. 7 The radial displacement (U_r) vs the radial stress (P_i (MPa) or $\sigma_{rr(j)}$) by Alejano *et al.* (2010) and proposed methods for different quality of rock mass

rational approach and uses an analytical type calculation. It is based on the analysis of the stress and strain state that develops in the rock around a tunnel. It can be profitably used for the estimation of the loads that act on the support structures, of the thickness of the plastic zone at the tunnel boundary, of the expected convergences (Oreste 2009).

The convergence-confinement curve (or GRC) basically consists of the definition of the internal pressure (radial stress)-radial displacement (in absolute values) relationships on the boundary of a circular void that represents the tunnel (Fig. 6).

Appendix A sets out the stepwise sequence of calculations to obtain ground response curve, based on the proposed approach.

4. Application examples

To evaluate the efficiency of the proposed method, first of all, some examples are selected from Alejano *et al.* (2010) (which was quantitatively verified by other methods and had exact predictions). The input data of the examples are available in Table 1.

Figs. 7 and 8. show ground response curves (GRC) (the radial displacement vs. the radial stress) and the corresponding plastic radius, respectively; predicted by the Alejano *et al.* (2010) method and by the analytical proposed method for different quality of rock mass. Table 2 shows the exact maximum values of the displacements and the plastic radii for each case.

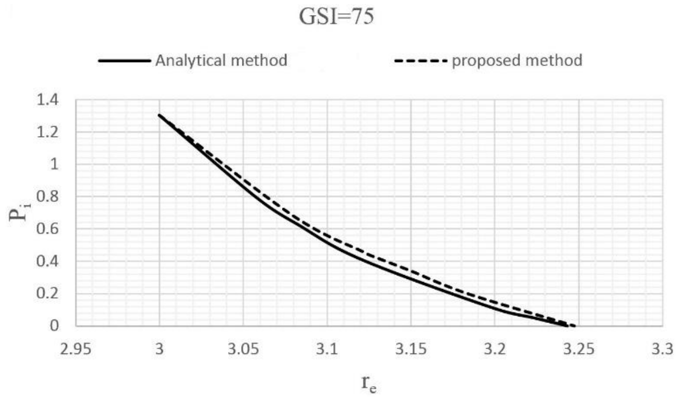

(a) GSI = 75

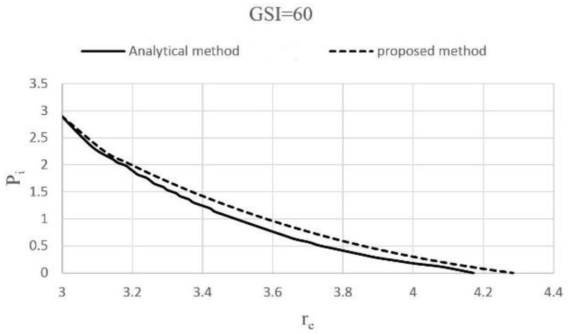

(b) GSI = 60

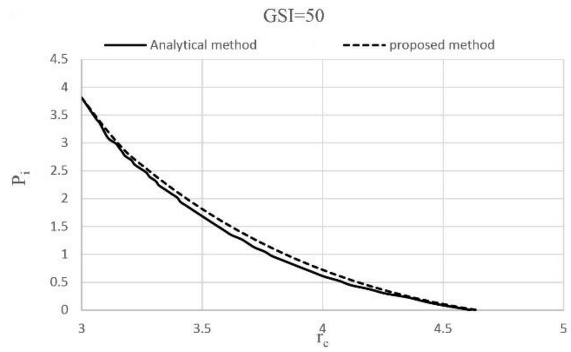

(c) GSI = 50

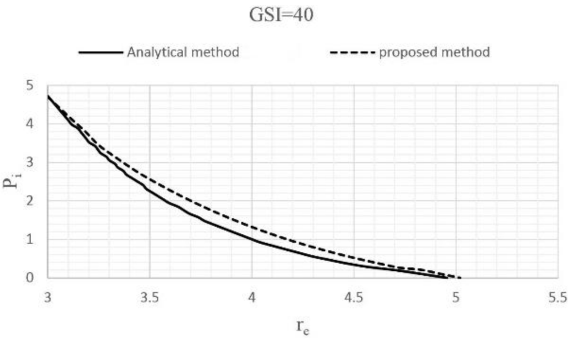

(d) GSI = 40

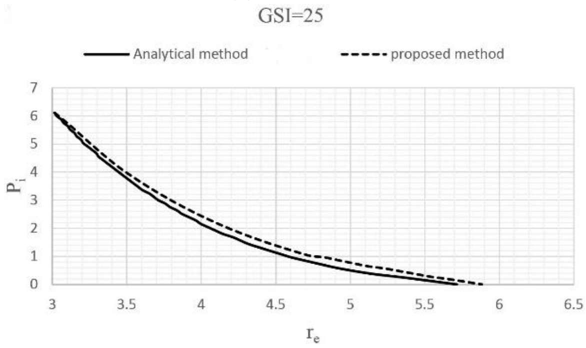

(e) GSI = 25

Fig. 8 The plastic radius r_e (m) vs the radial stress (P_i (MPa) or $\sigma_{rr(j)}$) by Alejano *et al.* (2010) and proposed methods for different quality of rock mass

Table 2 Plastic radius and the maximum radial displacement of proposed and Alejano *et al.* (2010) methods

	GSI = 75	GSI = 70	GSI = 60	GSI = 50	GSI = 40	GSI = 30	GSI = 25
Plastic radius, re (m) (proposed method)	3.24	3.804	4.28	4.64	5.02	5.43	5.88
Plastic radius, r_e (m) (Alejano *et al.* 2010)	3.22	-	4.2	4.65	4.96	-	5.735
The max. dis., $u_{r\,max}$ (mm) (proposed method)	1.8	3.44	7.6	15.62	28.16	49.34	78.05
The max. dis., $u_{r\,max}$ (mm) (Alejano *et al.* 2010)	1.7	-	7.3	15	27.4	-	75.3

Table 3 Characteristic of different quality of rock mass (Park *et al.* 2008)

	Case 1	Case 2	Case 3
Young's Modulus, **E** (MPa)	1380	40000	480
Poisson's ratio, ν	0.25	0.2	0.25
Initial stress, $\mathbf{p_0}$ (MPa)	3.31	108	5

Table 3 Continued

	Case 1	Case 2	Case 3
Radius of tunnel, $\mathbf{r}_i$ (m)	5.35	4	5
σ_c (MPa)	30	300	7.5
m_p	4.5	7.5	0.55
s_p	0.02	0.1	0
m_r	0.45(*1)	1.0	0.55
s_r	0.002(*1)	0.01	0
φ_p	40	55	22.4
ψ_{peak}	5	13.75	0
ψ_r	0	0	0
η^*	0.004742	0.004	0.01

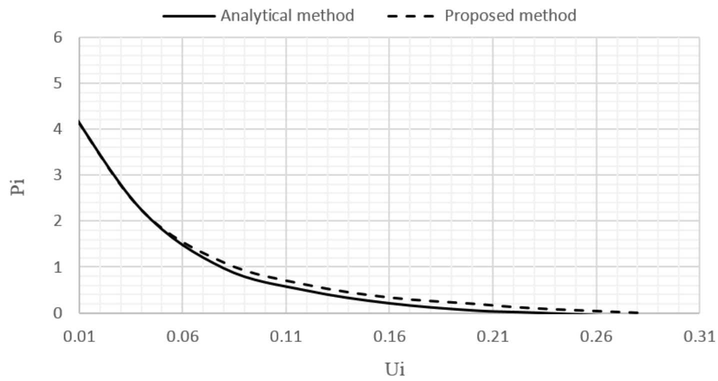

(a) Case 1

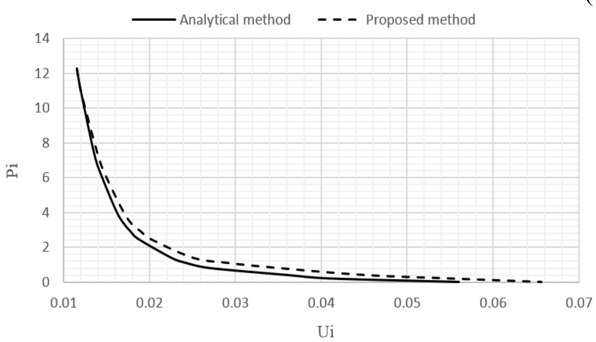

(b) Case 2

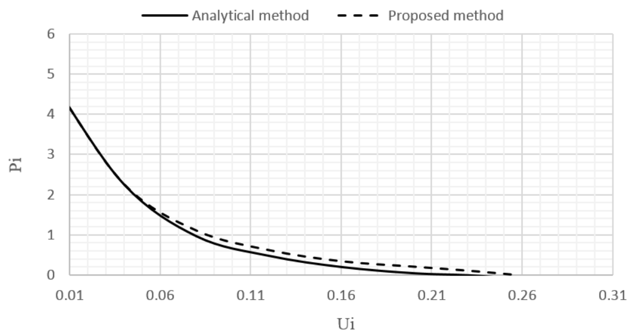

(c) Case 3

Fig. 9 The radial displacement (U_r) vs the radial stress (P_i (MPa) or $\sigma_{rr(j)}$) by Park *et al.* (2008) and the proposed methods for different quality of rock mass

Table 4 Plastic radius and the maximum radial displacement of proposed and Park *et al.* (2008) methods

	Case 1	Case 2	Case 3
Plastic radius, re (m) **(proposed method)**	19.53	8.96	18.05
Plastic radius, r_e (m) **(Park *et al.* 2008)**	19.21	8.76	17.85
The max. dis., $u_{r\,max}$ (mm) **(proposed method)**	28.1	6.56	25.5
The max. dis., $u_{r\,max}$ (mm) **(Park *et al.* 2008)**	27.3	5.6	23

In continue, more examples are solved from Park *et al.* 2008. The Input data and the results are now available in Table 3, and results are Fig. 9, and Table 4, respectively.

As observed, the predictions of proposed method, by using the elastoplastic stiffness matrix are in good agreement with those of the other analytical approaches. Furthermore, due to plane strain condition, using of 3D Hoek-Brown failure criterion does not have any advantage over conventional 2D failure criterion.

5. Relationship between a tunnel convergence and the uniaxial strength of rock mass

Hoek (1999) showed that the ratio of the uniaxial compressive strength of the rock mass σ_{cm} to the in-situ stress p_0 can be used as an indicator of potential tunnel squeezing problems. Then, Hoek and Marinos (2000) presented a relationship between the squeezing potential

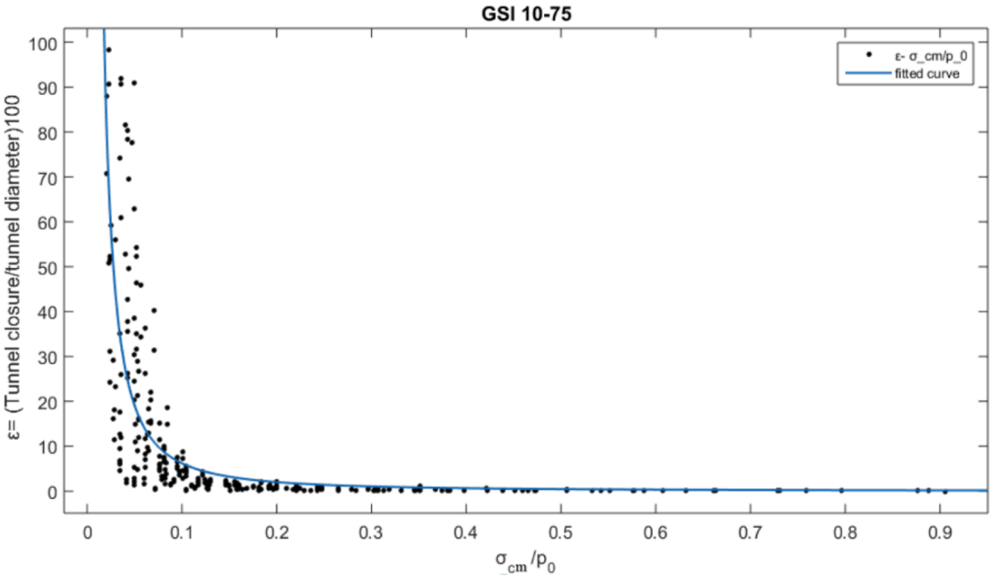

Fig. 9 Unsupported tunnel convergence against the ratio of rock mass strength to in situ stress, obtained by using the proposed approach

and the percentage "strain" of the tunnel i.e,. the ratio of tunnel closure to tunnel diameter.

For this purpose, a wide range of conditions for the effective parameters (including rock mass and tunnel properties) were considered. But, a small range for the Geological Strength Index i.e., 10 < GSI < 35 was assumed which is representative of poor rock mass quality showing typically the elastic-perfectly plastic stress-strain law. As a result, Duncan Fama (1993), and Carranza-Torres and Fairhurst (1999) approaches were used to obtain data to present the relationship. Furthermore, these approaches had not been developed according to the modified Hoek-Brown failure criterion (Hoek *et al.* 2002) nor the Elasticity Modulus by Hoek and Diederichs (2006).

Therefore, based on the method presented, it is worth developing a relationship for different rock mass quality exhibiting different post-failure stress-strain behavior, and updating it according to the recent advances. Fig. 10 gives the analyses result of all of tunnel cases following a clearly defined pattern. The fitted relationship is

$$\varepsilon = 0.036\left(\frac{\sigma_{cm}}{p_0}\right)^{-1.958} \qquad \mathrm{R-square} = 0.9986 \quad \text{(by Matlab)} \tag{41}$$

where $\sigma_{cm} = s_p{}^{a}\sigma_{ci}$

This relationship is for the conditions of a circular tunnel in a hydrostatic stress field which are seldom met in the field. As Hoek and Marinos (2000) stated, while these predictions are acceptably accurate for application to actual tunnels and for preliminary design, there remains a need to use a more sophisticated method of analysis for final design.

6. Conclusions

This study presented a new analytical-numerical procedure to calculate the stresses and strains around a circular tunnel subjected to a hydrostatic stress in-situ stress. The circular plastic zone meshed into annular rings, and the calculations started from the tunnel wall by incrementing the stresses (from the initial values prior to excavation to the final values after excavation) and the corresponding strains increments were obtained. An elastic-plastic stiffness matrix was used in which the 3D Hoek-Brown failure criterion (Ziang and Zhao 2015) and 3D the Mohr-Coulomb stress function as potential function were employed, respectively. The calculation procedures can be repeated for the next rings where the final status of stresses is found by the stress equilibrium differential equation through using the finite difference method.

The predicted results by the proposed approach for different rock mass quality (exhibiting different post-failure stress-strain behavior) were in good agreement with those of other well-known analytical approaches.

Finally, according to the predicted results data, a relationship was proposed to give the closure of the tunnel in terms of uniaxial strength of the rock mass and of tunnel depth.

References

Alejano, L.R. and Alonso, E. (2005), "Considerations of the dilatancy angle in rocks and rock masses", *Int. J. Rock Mech. Min. Sci.*, **42**(4), 481-507. https://doi.org/10.1016/j.ijrmms.2005.01.003.

Alejano, L.R., Alonso, E., Rodriguez-Dono, A. and Fernandez-Manin, G. (2010), "Application of the convergence-confinement method to tunnels in rock masses exhibiting Hoek–Brown strain-softening behavior", *Int. J. Rock Mech. Min. Sci.*, **1**(47), 150-160. https://doi.org/ 10.1016/j.ijrmms.2009.07.008.

Alejano, L.R., Rodriguez-Dono, A., Alonso, E. and Manín, G.F. (2009), "Ground reaction curves for tunnels excavated in different quality rock masses showing several types of post-failure behavior", *Tunn. Undergr. Sp. Technol.*, **24**(6), 689-705. https://doi.org/10.1016/j.tust.2009.07.004.

Alonso, E., Alejano, L.R., Varas, F., Fdez-Manin, G. and Carranza-Torres, C. (2003), "Ground response curves for rock masses exhibiting strain-softening behavior", *Int. J. Numer. Anal. Meth. Geomech.*, **27**(13), 1153-1185. https://doi.org/10.1002/nag.315.

Brown, E.T., Bray, J.W., Ladanyi, B. and Hoek, E. (1983), "Ground response curves for rock tunnels", *J. Geotech. Eng.*, **109**(1), 15-39. https://doi.org/10.1061/(ASCE)0733-9410(1983)109:1(15).

Carranza-Torres, C. (1998), "Self-similarity analysis of the elasto-plastic response of underground openings in rock and effects of practical variables", University of Minnesota, Minnesota, U.S.A.

Carranza-Torres, C. (2004), "Elasto-plastic solution of tunnel problems using the generalized form of the Hoek-Brown failure criterion", *Int. J. Rock Mech. Min. Sci.*, **41**(S1), 1-11. https://doi.org/10.1016/j.ijrmms.2004.03.111.

Carranza-Torres, C. and Fairhurst, C. (1999), "The elasto-plastic response of underground excavations in rock masses that satisfy the Hoek-Brown failure criterion", *Int. J. Rock Mech. Min. Sci.*, **36**(6), 777-809. https://doi.org/10.1016/S0148-9062(99)00047-9.

Fahimifar, A. Ghadami, H. and Ahmadvand, M., (2015), "The ground response curve of underwater tunnels, excavated in a strain-softening rock mass", *Geomech. Eng.*, **8**(3), 323-359. https://doi.org/10.12989/gae.2015.8.3.323.

FAMA, M.E.D. (1993), *Numerical Modeling of Yield Zones in Weak Rock*, in *Analysis and Design Methods*, 49-75.

González-Cao, J., Varas, F., Bastante, F.G. and Alejano, L.R. (2013), "Ground reaction curves for circular excavations in non-homogeneous, axisymmetric strain-softening rock masses", *J. Rock Mech. Geotech. Eng.*, **5**(6), 431-442. https://doi.org/10.1016/j.jrmge.2013.08.001.

Griffiths, D.V. and Willson, S.M. (1986), "An explicit form of the plastic matrix for a Mohr-Coulomb material", *Commun. Appl. Numer. Meth.*, **2**(5), 523-529. https://doi.org/10.1002/cnm.1630020511.

Hoek, E. (1999), "Putting numbers to geology—an engineer's viewpoint", *Quart. J. Eng. Geol. Hydrogeol.*, **32**(1), 1-19. https://doi.org/10.1144/GSL.QJEG.1999.032.P1.01.

Hoek, E. and Brown, E.T. (1997), "Practical estimates of rock mass strength", *Int. J. Rock Mech. Min. Sci.*, **34**(8), 1165-1186. https://doi.org/10.1016/S1365-1609(97)80069-X.

Hoek, E. and Diederichs, M.S. (2006), "Empirical estimation of rock mass modulus", *Int. J. Rock Mech. Min. Sci.*, **43**(2), 203-215. https://doi.org/10.1016/j.ijrmms.2005.06.005.

Hoek, E. and Marinos, P. (2000), "Predicting tunnel squeezing problems in weak heterogeneous rock masses", *Tunn. Tunn. Int.*, **32**(11), 45-51.

Hoek, E., Carranza-Torres, C. and Corkum, B. (2002), "Hoek-Brown failure criterion-2002 edition", *Proc. NARMS-Tac*, **1**(1), pp.267-273.

https://doi.org/10.1016/j.tust.2017.11.004.

Jiang, H. and Xie, Y.L. (2012), "A new three-dimensional Hoek-Brown strength criterion", *Acta Mechanica Sinica*, **28**(2), 393-406. https://doi.org/10.1007/s10409-012-0054-2.

Jiang, H. and Zhao, J. (2015), "A simple three-dimensional failure criterion for rocks based on the Hoek Brown criterion", *Rock Mech. Rock Eng.*, **48**(5), 807-1819. https://doi.org/10.1007/s00603-014-0691-9.

Lai, W.M., Rubin, D.H., Krempl, E. and Rubin, D. (2009), *Introduction to Continuum Mechanics*, Butterworth-Heinemann.

Lee, Y.K. and Pietruszczak, S. (2008), "A new numerical procedure for elasto-plastic analysis of a circular opening excavated in a strain-softening rock mass", *Tunn. Undergr. Sp. Technol.*, **23**(5), 588-599. https://doi.org/10.1016/j.tust.2007.11.002.

Nikadat, N. and Fatehi Marji, M., (2016), "Analysis of stress distribution around tunnels by hybridized FSM and DDM considering the influences of joints parameters", *Geomech. Eng.*, **11**(2), 269-288. https://doi.org/10.12989/gae.2016.11.2.269.

Oreste, P. (2009), "The convergence-confinement method: roles and limits in modern geomechanical tunnel design", *Amer. J. Appl. Sci.*, **6**(4), 757. https://doi.org/10.3844/ajassp.2009.757.771.

Osguii, R. and Oreste, P. (2007), "Convergence-control approach for rock tunnels reinforced by grouted bolts, using the homogenization concept", *Geotech. Geol. Eng.*, **25**(4), 431-440. https://doi.org/10.1007/s10706-007-9120-0.

Panet, M. (1993), *Understanding Deformations in Tunnels*, in *Comprehensive Rock Engineering*, Pergamon Press, **1**, 663-690.

Paraskevopoulou, C. and Diederichs, M. (2018), "Analysis of time-dependent deformation in tunnels using the convergence-confinement method", *Tunn. Undergr. Sp. Technol.*, **71**, 62-80. http://doi.org/10.1016/j.tust.2017.07.001.

Park, K. (2017), "Simple solutions of an opening in elastic-brittle plastic rock mass by total strain and incremental approaches", *Geomech. Eng.*, **13**(4), 585-600. https://doi.org/10.12989/gae.2017.13.4.585.

Park, K.H. and Kim, Y.J. (2006), "Analytical solution for a circular opening in an elastic-brittle-plastic rock", *Int. J. Rock Mech. Min. Sci.*, **43**(4), 616-622. https://doi.org/10.1016/j.ijrmms.2005.11.004.

Park, K.H., Tontavanich, B. and Lee, J.G. (2008), "A simple procedure for ground response curve of circular tunnel in elastic-strain softening rock masses", *Tunn. Undergr. Sp. Technol.*, **23**(2), 151-159. https://doi.org/10.1016/j.tust.2007.03.002.

Potts, D.M., Zdravkovic, L. and Zdravković, L. (2001), *Finite Element Analysis in Geotechnical Engineering: Application (Vol. 2)*, Thomas Telford.

Quevedo, F. and Bernaud, D. (2018), "Parametric study of the convergence of deep tunnels with long term effects: Abacuses", *Geomech. Eng.*, **15**(4), 973-986. https://doi.org/10.12989/gae.2018.15.4.973.

Ranjbarnia, M., Fahimifar, A. and Oreste, P. (2015), "Analysis of non-linear strain-softening behaviour around tunnels", *Proc. Inst. Civ. Eng. Geotech. Eng.*, **168**(1), 16-30. https://doi.org/10.1680/geng.13.00144.

Sadd, M.H. (2009), *Elasticity: Theory, Applications, and Numeric*, Academic Press.

Sharan, S.K., (2003), "Elastic-brittle-plastic analysis of circular openings in Hoek-Brown media", *Int. J. Rock Mech. Min. Sci.*, **40**(6), 817-824. https://doi.org/10.1016/S1365-1609(03)00040-6.

Tu, H., Qiao, C. and Han, Z. (2018), "Elastic-brittle-plastic analysis of the radial subgrade modulus for a circular cavity based on the generalized nonlinear unified strength criterion", *Tunn. Undergr. Sp. Technol.*, **71**, 623-636. https://doi.org/10.1016/j.tust.2017.11.004.

Wang, F. and Zou, J.F. (2018), "A simple prediction procedure of strain-softening surrounding rock for a circular opening", *Geomech. Eng.*, **16**(6), 619-626. https://doi.org/10.12989/gae.2018.16.6.619.

Wang, Sh., Yin, X., Tang, H. and Ge, X. (2010), "A new approach for analyzing circular tunnel in strain-softening rock mass", *Int. J. Rock Mech. Min. Sci.*, **47**(1), 170-178. https://doi.org/10.1016/j.ijrmms.2009.02.011.

Yoo, C. (2016), "Effect of spatial characteristics of a weak zone on tunnel deformation behavior", *Geomech. Eng.*, **11**(1), 41-58. https://doi.org/10.12989/gae.2016.11.1.041.

Zareifard, M.R. (2019), “Ground response curve of deep circular tunnel in rock mass exhibiting Hoek-Brown strain-softening behaviour considering the dead weight loading”, *Eur. J. Environ. Civ. Eng.* https://doi.org/10.1080/19648189.2019.1632745.

Zhuang, P.Z. and Yu, H.S. (2018), “A unified analytical solution for elastic–plastic stress analysis of a cylindrical cavity in Mohr-Coulomb materials under biaxial in situ stresses”, *Géotechnique*, **69**(4), 369-376. https://doi.org/10.1680/jgeot.17.P.281.

Zou, J.F. and Wei, X.X. (2018), “An improved radius-incremental-approach of stress and displacement for strain-softening surrounding rock considering hydraulic-mechanical coupling”, *Geomech. Eng.*, **16**(1), 59-69. https://doi.org/10.12989/gae.2018.16.1.059.

Zou, J.F. and Zheng, H. (2016), ‘‘Numerical approach for strain-softening rock with axial stress”, *Proc. Inst. Civ. Eng. Geotech. Eng.*, **169**(3), 276-290. https://doi.org/10.1680/jgeen.15.00097.

Zou, J.F., Li, C. and Wang, F. (2017), “A new procedure for ground response curve (GRC) in strain-softening surrounding rock”, *Comput. Geotech.*, **89**, 81-91. https://doi.org/10.1016/j.compgeo.2017.04.009.

Zou, J.F., Yang, T., Ling, W., Guo, W. and Huang, F. (2019), “A numerical stepwise approach for cavity expansion problem in strain-softening rock or soil mass”, *Geomech. Eng.*, **18**(3), 225-234. https://doi.org/10.12989/gae.2019.18.3.225.

CC

Appendix A. The stepwise procedures to calculate GRC and Plastic radius

Preliminary Calculations

(1) Find σ_{re} from $2(p_0 - \sigma_{re}) = \sigma_{ci}\left(m_p \frac{\sigma_{re}}{\sigma_{ci}} + s_p\right)^a$ by implicit way.

(2) $\sigma_{r1} = \sigma_{re}$

(3) $\sigma_{\theta 1} = 2p_0 - \sigma_{r1}$

(4) $\sigma_y = p_0$ (constant for all indices)

(5) $\sigma_{r\theta} = 0$ (constant for all indices)

(6) $\varepsilon_{\theta 1} = \varepsilon_{\theta e} = \frac{1}{2G}[(1-\nu)(\sigma_{\theta 1} - p_0) - \nu(\sigma_{r1} - p_0)]$

ν is Poisson's ratio.

(7) $\varepsilon_{r1} = \varepsilon_{re} = \frac{1}{2G}[(1-\nu)(\sigma_{r1} - p_0) - \nu(\sigma_{\theta 1} - p_0)]$

(8) $\varepsilon^p_{\theta(1)} = 0$ (plastic tangential strain in the first step)

(9) $\varepsilon^p_{r(1)} = 0$ ((plastic radial strain in the first step)

(10) $m_1 = m_p, s_1 = s_p, \overline{\psi}_1 = \psi_p$, $a_1 = a_p$, $c'_1 = c'_p$, $\varphi'_1 = \varphi'_p$ (peak value)

(11) $d\sigma_{rr} = \sigma_{re}/(n-1)$; n is number of increments in each ring and is assumed as an arbitrary value.

(12) $d\sigma_{yy} = d\sigma_{r\theta} = 0$

Sequence of calculation for each ring

(1) $\sigma_{r(j+1)} = \sigma_{r(j)} - d\sigma_{rr}$ (for first step, $\sigma_{r(j)} = \sigma_{r1}$)

(2) Find $\sigma_{\theta(j+1)}$ from equations of below box (i.e., 3D Hoek- Brown failure criterion) by implicit way

$$\sigma'_m = \frac{1}{3}\left(\sigma_{\theta(j+1)} + \sigma_{r(j+1)} + \sigma_{y(j+1)}\right)$$

$$\sqrt{J'_2} = \sqrt{\frac{1}{6}\left[\left(\sigma_{\theta(j+1)} - \sigma_{y(j+1)}\right)^2 + \left(\sigma_{\theta(j+1)} - \sigma_{r(j+1)}\right)^2 + \left(\sigma_{y(j+1)} - \sigma_{r(j+1)}\right)^2\right]}$$

$$\theta_{j+1} = \mathrm{Arccos}\left(\frac{2\sigma_{\theta(j+1)} - \sigma_{y(j+1)} - \sigma_{r(j+1)}}{2\sqrt{3}\sqrt{J'_2}}\right)$$

$$A(\theta_{j+1}) = 2\cos\left(\frac{\pi}{3} - \theta_{j+1}\right)$$

$$f(\{\sigma'\},\{m\}) = \frac{1}{m_{(j)}\sigma_{ci}^{1/a_{(j)}-1}}\left(\sqrt{3J'_2}\right)^{1/a_{(j)}} + \frac{A(\theta_{(j+1)})}{\sqrt{3}}\sqrt{J'_2} - \frac{s_{(j)}\sigma_{ci}}{m_{(j)}} - \sigma'_m$$

(3) $d\sigma_{\theta\theta} = \sigma_{\theta(j+1)} - \sigma_{\theta(j)}$ (for first step, $\sigma_{\theta(j)} = \sigma_{\theta 1}$)

(4) $d\sigma_{mn} = \begin{bmatrix} d\sigma_{\theta\theta} \\ d\sigma_{yy} \\ d\sigma_{rr} \\ d\sigma_{r\theta} \end{bmatrix}$

(5) Calculate the differential of failure criterion and potential function to the stresses according to the following box

$$\frac{\partial f}{\partial \sigma} = \frac{\partial f}{\partial \sqrt{J'_2}}\frac{\partial \sqrt{J'_2}}{\partial \sigma'} + \frac{\partial f}{\partial \sigma'_m}\frac{\partial \sigma'_m}{\partial \sigma'} + \frac{\partial f}{\partial A(\theta)}\frac{\partial A(\theta)}{\partial \sigma'}$$

$$\frac{\partial p}{\partial \sigma} = \frac{\partial p}{\partial J'_2}\frac{\partial J'_2}{\partial \sigma'} + \frac{\partial p}{\partial \sigma'_m}\frac{\partial \sigma'_m}{\partial \sigma'} + \frac{\partial p}{\partial a_{pp}}\frac{\partial a_{pp}}{\partial \sigma'}$$

$$g(\theta_{j+1}) = \frac{\sin\varphi'_{(j+1)}}{\cos\theta_{(j+1)} + \frac{\sin\theta_{(j+1)}\sin\varphi'_{(j+1)}}{\sqrt{3}}}$$

$$g_{pp}(\theta_{j+1}) = \frac{\sin\psi_{(j+1)}}{\cos\theta_{(j+1)} + \frac{\sin\theta_{(j+1)}\sin\psi_{(j+1)}}{\sqrt{3}}}$$

$$a_{pp} = \left(\frac{c'_{(j+1)}}{\tan\varphi'_{(j+1)}} + {\sigma'_m}^*\right)\frac{g(\theta_{j+1})}{g_{pp}(\theta_{j+1})} - \sigma'_m$$

$$H = -\left[\frac{\partial f}{\partial \varepsilon^p}\right]\left[\frac{\partial p}{\partial \sigma}\right]$$

(6) $[D^{ep}] = [D^e] - \frac{[D^e]\left[\frac{\partial p}{\partial \sigma}\right]\left[\frac{\partial f}{\partial \sigma}\right]^T[D^e]}{\left[\frac{\partial f}{\partial \sigma}\right]^T[D^e]\left[\frac{\partial p}{\partial \sigma}\right] + H}$

(7) $d\varepsilon_{kl} = \left(D^{ep}_{mnkl}\right)^{-1} d\sigma_{mn}$

(8) $d\varepsilon_{kl} = \begin{bmatrix} d\varepsilon_{\theta\theta} \\ d\varepsilon_{yy} \\ d\varepsilon_{rr} \\ d\varepsilon_{r\theta} \end{bmatrix}$

(9) $\varepsilon^p_{\theta(j+1)} = \varepsilon^p_{\theta(j)} + d\varepsilon_{\theta\theta}$

(10) $\varepsilon^t_{\theta(j+1)} = \varepsilon_{\theta e} + \varepsilon^p_{\theta(j+1)}$ (total tangential strain in increment *j*+1)

(11) $\varepsilon^p_{r(j+1)} = \varepsilon^p_{r(j)} + d\varepsilon_{rr}$

(12) $\varepsilon^t_{\theta(j+1)} = \varepsilon^e_r + \varepsilon^p_{r(j+1)}$ (total radial strain in increment *j*+1)

(13) $\eta_{j+1} = \varepsilon^p_{\theta(j+1)} - \varepsilon^p_{r(j+1)}$

(14)

$$\begin{cases} \text{If } \eta_{j+1} < \eta^*, \text{then } \overline{\psi}_{j+1} = \psi_p - (\psi_p - \psi_r)\frac{\eta_{j+1}}{\eta^*}, \quad m_{j+1} = m_p - (m_p - m_r)\frac{\eta_{j+1}}{\eta^*}, \\ s_{j+1} = s_p - (s_p - s_r)\frac{\eta_{j+1}}{\eta^*}, \quad a_{j+1} = a_p - (a_p - a_r)\frac{\eta_{j+1}}{\eta^*} \\ , c'_{j+1} = c'_p - (c'_p - c'_r)\frac{\eta_{j+1}}{\eta^*}, \varphi'_{j+1} = \varphi'_p - (\varphi'_p - \varphi'_r)\frac{\eta_{j+1}}{\eta^*} \\ \text{If } \eta_{j+1} \geq \eta^*, \text{then } \overline{\psi}_{j+1} = \psi_r, \quad m_{j+1} = m_r, \quad s_{j+1} = s_r, \ a_{j+1} = a_r, \\ c'_{j+1} = c'_r \ , \varphi'_{j+1} = \varphi'_r \end{cases}$$

(15)

$$\begin{cases} \text{If } \sigma_{r(j+1)} > p_i \text{ , then increase j by 1 and repeat the calculation sequence.} \\ \text{If } \sigma_{r(j+1)} < p_i, \text{then go to the next step.} \end{cases}$$

Note: p_i is the radial pressure.

(16) $u_r = \varepsilon^t_{\theta(j+1)} \times r_a$ (r_a is tunnel radius)

(17) Find the location of the next ring (i+1) i.e., r_{i+1}=1.01r_i (Consider $r_0 = r_a$)

(18) Use equilibrium equation (i.e., Eq. (28)) and the failure criterion to obtain p_i value (or $\sigma_{r(i)}$) of the ring (i+1).

(19) If $p_i > \sigma_{re}$, repeat steps (17) to (18), Otherwise go to step (20)

(20) The plastic radius is $r_e = r_{i+1}$